

A Pipe Insulation Test Apparatus for Use Below Room Temperature*

Kenneth E. Wilkes, Andre O. Desjarlais, Therese K. Stovall, David L. McElroy,
Kenneth W. Childs, and William A. Miller

Oak Ridge National Laboratory
P. O. Box 2008
Building 4508, MS 6092
Oak Ridge, Tennessee 37831-6092
(865) 574-5931
FAX (865)-576-3894

For presentation at the
Fourth Symposium on Insulation Materials
Charleston, South Carolina
October 21-22, 2002

*Research sponsored by the Office of Building Technology, State, and
Community Programs, U.S. Department of Energy under Contract No.
DE-AC05-00OR22725 with UT-Battelle, LLC.

"The submitted manuscript has
been authored by a contractor of
the U.S. Government under
Contract No. DE-AC05-
00OR22725. Accordingly, the U.S.
Government retains a nonexclusive,
royalty-free license to publish or
reproduce the published form of this
contribution, or allow others to do
so, for U. S. Government
purposes."

Kenneth E. Wilkes, Andre O. Desjarlais, Therese K. Stovall, David L. McElroy, Kenneth W. Childs, and William A. Miller¹

A Pipe Insulation Test Apparatus for Use Below Room Temperature

Reference: Wilkes, K. E., Desjarlais, A. O., Stovall, T. K., McElroy, D. L., Childs, K. W., and Miller, W. A., “**A Pipe Insulation Test Apparatus for Use Below Room Temperature,**” *Insulation Materials: Testing and Applications: 4th Volume, ASTM STP 1426*, A. O. Desjarlais, Ed., American Society for Testing and Materials, West Conshohocken, PA, 2002.

Abstract

Several ASTM material standards for pipe insulations require thermal performance data below room temperature. ASTM Test Method for Steady-State Heat Transfer Properties of Horizontal Pipe Insulation (C 335) and ASTM Test Method for Steady-State Heat Transfer Properties of Pipe Insulation Installed Vertically (C 1033) are the only ASTM pipe insulation test methods, but these are used above room temperature. This paper describes proof-of-concept tests near room temperature on a new pipe insulation tester for use below room temperature. It is a radial heat flow modification of ASTM Practice for Using a Guarded-Hot-Plate Apparatus or Thin-Heater Apparatus in the Single-Sided Mode (C 1044).

The pipe insulation test specimen is inside an electrically heated cylindrical screen which is guarded by a fluid-cooled copper shell with intervening insulation. The main heat flow is radially inward through the test specimen to a central fluid-cooled tube. By matching the temperature of the heater to that of the guard, unwanted radial heat flow to or from the screen heater is minimized.

The new tester has yielded results on three types of pipe insulation: fiberglass, polyisocyanurate foam, and elastomeric foam. Results on the latter two types were compared with results on board specimens of similar materials using ASTM Test Method for Steady-State Thermal Transmission Properties by Means of the Heat Flow Meter Apparatus (C 518).

Finite difference thermal modeling using the HEATING7 program was completed on the tester and showed potential errors should be less than 1%. Designs are in progress to allow use of the tester to temperatures as low as -190 °C (-310 °F).

Key Words: pipe insulation, test apparatus, below room temperature

¹Senior Researchers, Oak Ridge National Laboratory, Oak Ridge, TN 37831.

Introduction

Several ASTM material standards for pipe insulation require thermal performance data below room temperature. There are two ASTM pipe insulation test methods, C 335 and C 1033. Both of these are based on a heated pipe, with heat flow outwards, and both are generally for use above room temperature.

This paper describes a new pipe insulation tester for use below room temperature, wherein the heat flow is inwards towards a cold pipe. It is a radial heat flow modification of C 1044, which applies to single-sided operation of a guarded-hot-plate or thin-heater apparatus. The paper also gives results of proof-of-concept tests, design modeling, and plans for extending operation to cryogenic temperatures.

Apparatus

An apparatus was constructed that allows measurements on pipe insulation operating below room temperature. Figure 1 shows a cutaway schematic of the apparatus. Starting from the inside, the apparatus consisted of a tube through which cold fluid circulated, the test specimen, a thin screen heater, guard insulation, a temperature-controlled guard shell, and outer insulation. The temperatures of the heater and shell were matched so that the heat generated in the thin heater passed radially inwards through the test insulation to the cooled inner tube. The central section of the apparatus served as a metered section with end regions forming a passive guard.

A cold pipe or tube was located at the axis of the apparatus. The initial setup used a copper tube with an outside diameter of 34.9 mm (1.375 in.) and a length of 1.5 m

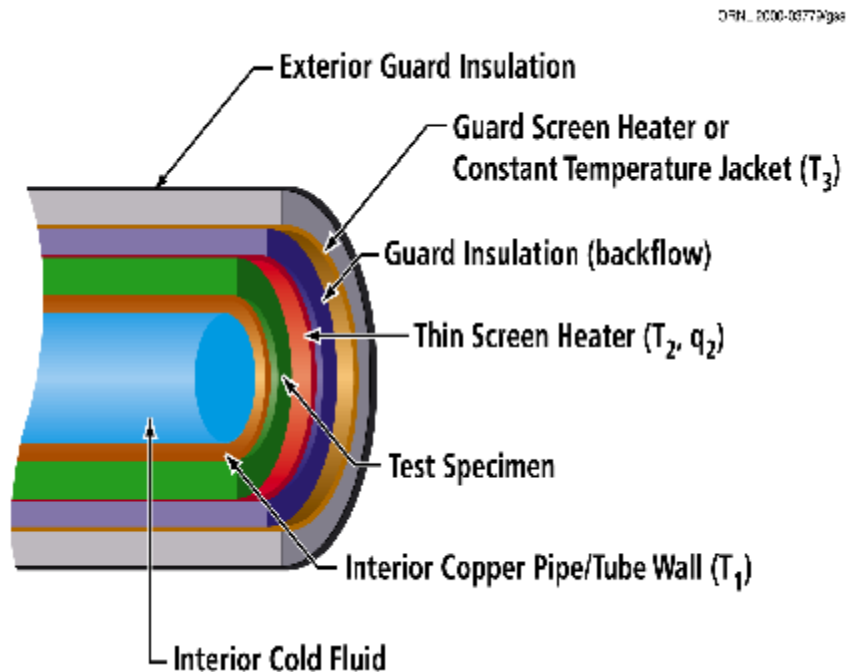


Figure 1 - Schematic of Pipe Insulation Test Apparatus for Below Room Temperature

(60 in.). Reducers and 12.7 mm (0.5 in.) outside diameter copper tubes were soldered at each end for attachment by rubber tubing to a constant temperature bath which circulated an ethylene glycol mixture through the tube. Initially, the tube was bare, but was later coated with Nextel paint to provide a total hemispherical emittance of 0.89.[1]

The thin heater was made of a nichrome screen having a 40 by 40 mesh (wires per 25.4 mm) of 0.25-mm-diameter wire (0.010 in. wire). This is the same type of heater that has been used for a flat thin-heater apparatus.[2] The screen was rolled into a cylinder with an inside diameter of 88.9 mm (3.50 in.), an outside diameter of 90.2 mm (3.55 in.), and a length of 0.946 m (37.25 in.). Heavy brass flanges were bolted to each end to provide distribution of a direct electrical current from a regulated D.C. power supply.

The outer shell was made from a Type M copper tube that had an outside diameter of 155.6 mm (6.125 in.), a wall thickness of 3.18 mm (0.125 in.), and a length of 0.914 m (36 in.). The tube was split lengthwise in half for convenience in assembly of the apparatus. Copper tubing with an outside diameter of 15.9 mm (0.625 in.) was soldered to the outside surfaces of the shell. The copper tubing was placed in a lengthwise serpentine pattern with four lengths of tubing on each half of the shell. The copper tubing was connected to a second constant temperature bath which circulated an ethylene glycol solution through the tubing. Initial tests were done with a bare copper inner surface, but a coating of Nextel paint (emittance of 0.89) was added later.

Glass fiber pipe insulation wrapped with silicone rubber sheets filled the space between the thin heater and the outer shell. Foil-faced glass fiber duct insulation about 25 mm thick was wrapped around the outside of the outer shell assembly. Finally, glass fiber batt insulation was placed around the portions of the cold tube that protruded from the ends of the test specimen.

Temperatures in the system were measured with Type E (chromel-constantan) thermocouples made from spools of calibrated 36 AWG (0.13 mm, 0.005 in. diameter) wire. An ice-water bath was used as a reference junction, and emfs were read from a calibrated digital voltmeter. On the 0.1 V range, the voltmeter had an accuracy of $\pm(0.08\mu\text{V} + 0.0013\%)$. Thermocouples were bonded to the copper surfaces using thermally conductive epoxy and were spot-welded to platinum wire studs that had been spot-welded to the thin heater. For the initial setup, thermocouples were mounted on the inner tube 0.43 m (17 in.) on each side of the midplane. After the inner tube was coated with Nextel paint, a thermocouple was added at its midplane. Five thermocouples were mounted on the heater: at the midplane, 0.23 m (9.0 in.) on each side of the midplane, and 0.34 m (13.5 in.) on each side of the midplane. One thermocouple was mounted on the inner surface of each half of the outer copper shell.

Power input to the thin heater was measured using voltage taps spot-welded at 0.23 m (9.0 in.) on each side of the midplane. The voltage taps were made of 22 AWG (0.64 mm, 0.025 in. diameter) nichrome wire. Use of nichrome wire essentially eliminated Seebeck emfs due to differences in temperature on the heater between the locations of the voltage taps. The current through the heater was measured by the voltage drop across a precision 0.01 ohm standard resistor in series with the heater. The power input to the 0.46 m (18.0 in.) long metering section was calculated as the product of the voltage drop and the current.

The apparent thermal conductivity (λ) of the test insulation was calculated from the following equation,

$$\lambda = \frac{P \ln(D_2/D_1)}{2\pi L (T_2 - T_1)} \quad (1)$$

where P is the power dissipated in the central 0.46 m (18.0 in.) metering section of the heater, L is the length of the metering section, 0.46 m (18.0 in.), D_1 and D_2 are the inside and outside diameters of the test insulation, respectively, and T_1 and T_2 are the inside and outside temperatures of the insulation, respectively. The temperature of the inside of the insulation was taken as the average of the readings of the thermocouples on the inner tube. When the test insulation fitted snugly inside the thin heater, the temperature of the outside of the insulation was taken as the average of the three middle thermocouples on the screen heater. If the test insulation did not fit snugly within the heater, additional thermocouples were taped to the outer surface of the test specimen at the same axial locations as the thermocouples on the heater.

The measured power was corrected for small heat exchanges between the heater and the outer copper shell. The average thermal conductivity of the insulation between these two components was measured in calibration tests by matching the temperature of the inner copper tube to that of the heater and then running the outer copper shell at a lower temperature. The measured value of apparent thermal conductivity was 0.0369 W/m·K, and this value was used for calculating corrections. Correction for this radial heat flow was less than 3%. No corrections were made for axial conduction along the heater since modeling described later in this paper shows this effect to be negligible.

A determinate uncertainty analysis was performed for the quantities in Eqn. 1. The maximum uncertainty (sum of absolute values of individual uncertainties) was estimated to be $\pm 1.7\%$ for the typical case of an insulation with outside and inside diameters of 88.9 mm (3.50 in.) and 34.9 mm (1.375 in.), respectively, and for a temperature difference of 20 °C. The most probable uncertainty (the square root of the sum of the squares of the individual uncertainties) was $\pm 0.8\%$ for the same case. These uncertainties will be different for other insulation sizes and temperature differences.

Test Results

Glass Fiber Insulation

The first set of measurements was made on a molded glass fiber pipe insulation that was obtained from the ORNL insulation shop. It had outside and inside diameters of 88.9 mm (3.50 in.) and 34.9 mm (1.375 in.), respectively. The density was 56 kg/m³ (3.5 lb/ft³). One set of tests was performed with bare copper surfaces on the central tube and on the outer shell, while the second set was performed after both of these surfaces had been blackened with a Nextel coating. Also, the midplane thermocouple was added to the inner tube during the painting operation. All subsequent testing on other types of

insulation was performed with blackened surfaces, and with three thermocouples on the inner tube.

Tests were performed with a temperature difference of 10 or 20 °C, and the results are shown in Figure 2. Blackening the tube resulted in an increase in the measured apparent thermal conductivity of about 4 to 5%. The data for the black tube were fitted to a relationship linear in temperature and the resulting equation is given on Figure 2 (it is recognized that thermal conductivity generally varies more strongly with temperature, but a linear variation is adequate over the small temperature range shown in Figure 2). The individual data points are all within 1% of the regression line. ASTM Specification for Mineral Fiber Pipe Insulation (C 547) lists the maximum apparent thermal conductivity at 37.8 °C for Type I pipe insulation (minimum 48 kg/m³, 3 lb/ft³) as 0.0361 W/m·K. The linear regression of the data with the black tube is less than 5% below this value.

It was also observed that blackening the tube produced more uniform temperatures within the system. Before blackening, temperature variations on the inner tube ranged from 0.30 to 0.92 °C (the larger variations corresponded to larger temperature differences across the test insulation). After blackening, these variations were reduced to 0.21 to 0.50 °C. Similarly, temperature variations on the screen varied from 0.10 to 0.24 °C before blackening, and 0.02 to 0.10 °C after blackening.

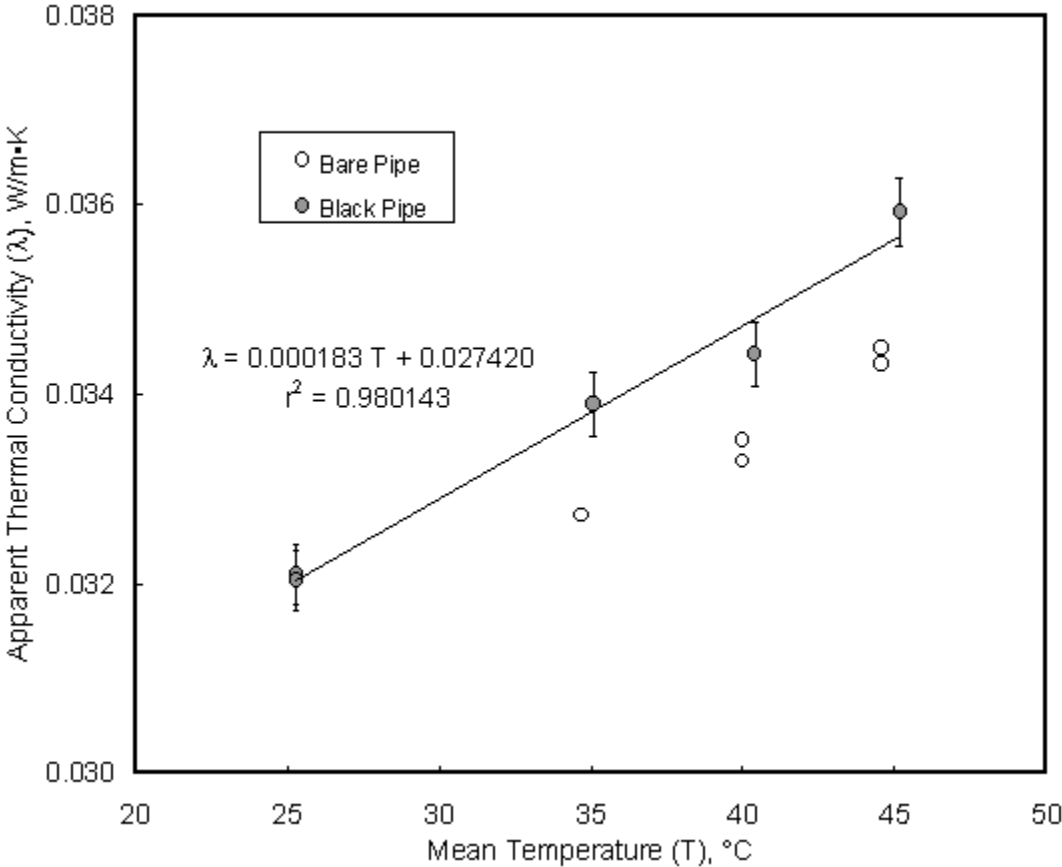


Figure 2 - Apparent Thermal Conductivity of Glass Fiber Pipe Insulation. The error bars on the data points for the black pipe represent a variation of ±1%.

Polyisocyanurate Foam Insulation

The second series of tests was performed on polyisocyanurate foam insulation furnished by an insulation manufacturer. The two-piece pipe insulation had outside and inside diameters of 88.9 mm (3.50 in.) and 34.9 mm (1.375 in.), respectively. Three companion flat slabs about 23.8 mm (0.937 in.) thick were cut from the same piece of foam that was used for the pipe insulation. The density of the flat slabs was measured as 33 kg/m³ (2.1 lb/ft³). The apparent thermal conductivity of the flat slabs was measured using C 518 to provide a basis for comparison with results from the pipe insulation tester.

Since the foam was still aging, apparent thermal conductivity measurements were made over a time period of six to eight months. Measurements were made at a mean temperature of 25 °C (77 °F) with a temperature difference of 20 °C. Figure 3 shows the normalized apparent thermal conductivity versus time for the average of the three boards and for the pipe insulation. The data were normalized by dividing the actual thermal conductivity values by the first value that was measured for the pipe insulation. The aging time was estimated by the time of receipt of the specimens. Over the time period of the measurements, the apparent thermal conductivities of both the board and pipe insulations increased by about 8%. Figure 4 shows the apparent thermal conductivity

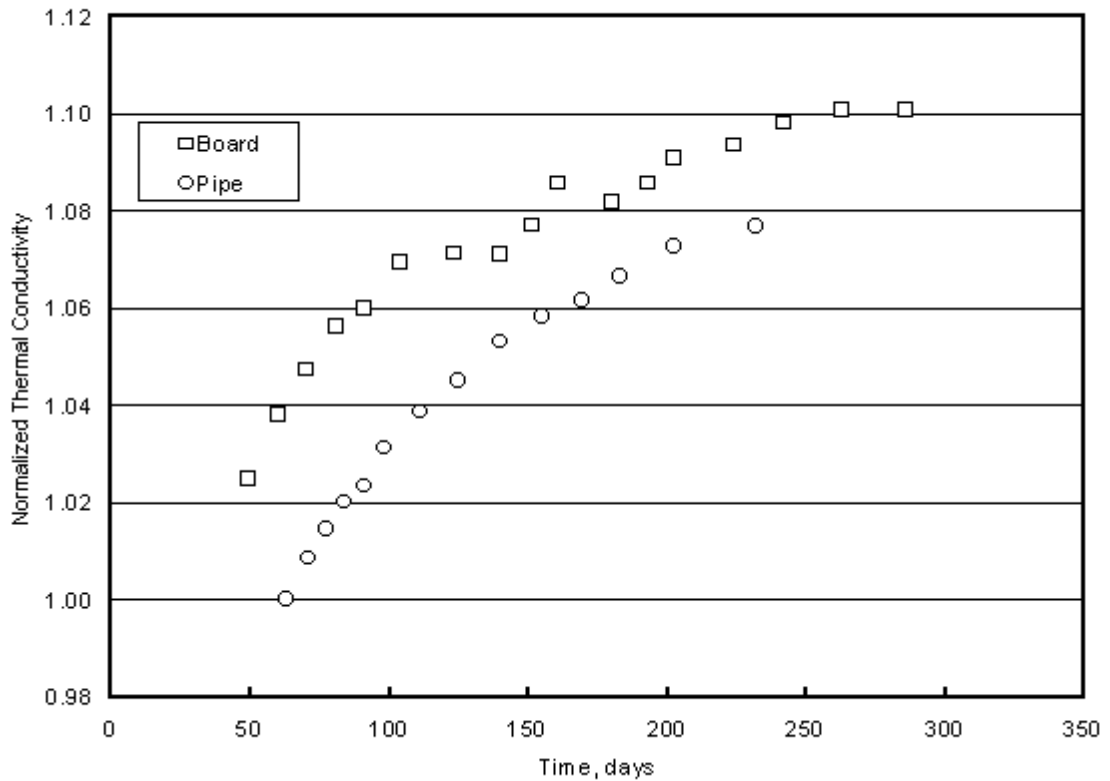


Figure 3 - *Apparent Thermal Conductivity of Polyisocyanurate Foam Insulation. The data have been normalized by dividing each data point by the first data point for the pipe insulation.*

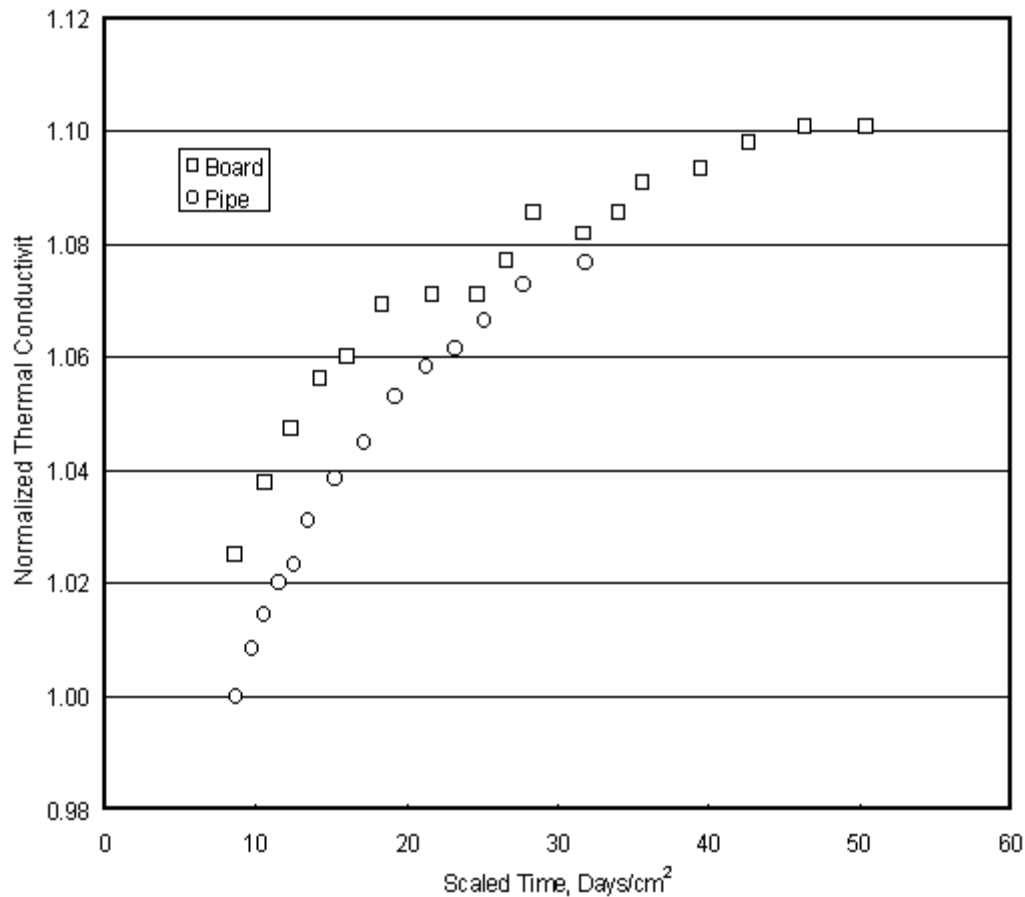


Figure 4 - *Apparent Thermal Conductivity of Polyisocyanurate Foam Insulation. The data have been normalized by dividing each data point by the first data point for the pipe insulation. The scaled time is the aging time divided by the square of the board thickness or the square of the pipe insulation wall thickness.*

plotted versus a scaled time, which was obtained by dividing the aging time by the square of either the board thickness or the square of the pipe insulation wall thickness. Plotting the data versus scaled time brings the two curves closer together. When compared this way, the two conductivities are within about 2% initially and then converge to within about 1%.

The level of agreement between the two sets of data is considered to be very good, especially considering that the previous aging history of the specimens and their relative locations within the piece from which they were cut were not known. In addition, the different geometries of the specimens may produce differences in aging. For the board specimens, diffusion of air into the specimen and diffusion of the blowing agent out should be one-dimensional in the central location where the apparent thermal conductivity was measured. For the pipe specimen, however, two-dimensional diffusion should occur because of the cut radial surfaces. Further study is needed to determine the impact of the two-dimensional diffusion on the average apparent thermal conductivity of pipe insulation specimens.

Elastomeric Foam Insulation

The third set of measurements was performed on elastomeric foam pipe insulation. The pipe insulation was obtained from the ORNL insulation shop. It had outside and inside diameters of 80.4 mm (3.167 in.) and 28.6 mm (1.125 in.), respectively. The density was 66 kg/m³ (4.1 lb/ft³). The previously used inner copper tube was replaced with a blackened copper tube having an outside diameter of 28.6 mm (1.125 in.) to accommodate the new specimen. Three thermocouples were taped to the outside surface of the insulation, at the midplane and at 0.23 m (9 in.) on each side of the midplane. Silicone rubber sheets were wrapped around the specimen to fill the remaining space between the thin heater and the specimen. The thermal resistances of the specimen and silicone rubber were such that about 90% of the 25 °C temperature difference between the heater and the inner tube occurred across the test specimen.

To form a basis for comparison, heat-flow-meter apparatus measurements were performed on flat sheets of similar elastomeric foam insulation from which the skins had been removed. The sheets were about 7.6 mm (0.3 in.) thick, and four sheets were stacked to make up a test specimen. The density of the sheet material was 61 kg/m³ (3.8 lb/ft³), which was within 10% of the density of the pipe insulation.

Results of the measurements on the pipe insulation are given in Table 1, in the order in which the tests were performed. Table 1 lists the deviation from a linear regression of the apparent thermal conductivity versus mean temperature. This shows that repeat tests at a given temperature agree within about 1%. Generally, slightly lower apparent thermal conductivities were obtained after performing tests at colder pipe temperatures, perhaps because of a slight drying of the material.

Figure 5 compares the apparent thermal conductivity of the pipe insulation with that of the sheet material, and also with values listed in ASTM Specification for

Table 1 - Results of Measurements on Elastomeric Foam Pipe Insulation. The data are listed in the order in which they were measured.

Pipe Temp., °C	Mean Temp., °C	λ , W/m·K	Deviation from Regression, %
15.8	24.3	0.03966	+0.5
5.5	14.2	0.03811	+0.6
15.3	24.1	0.03950	+0.1
10.4	19.2	0.03865	-0.07
0.6	9.3	0.03710	-0.06
5.5	14.2	0.03773	-0.4
15.3	24.1	0.03920	-0.6

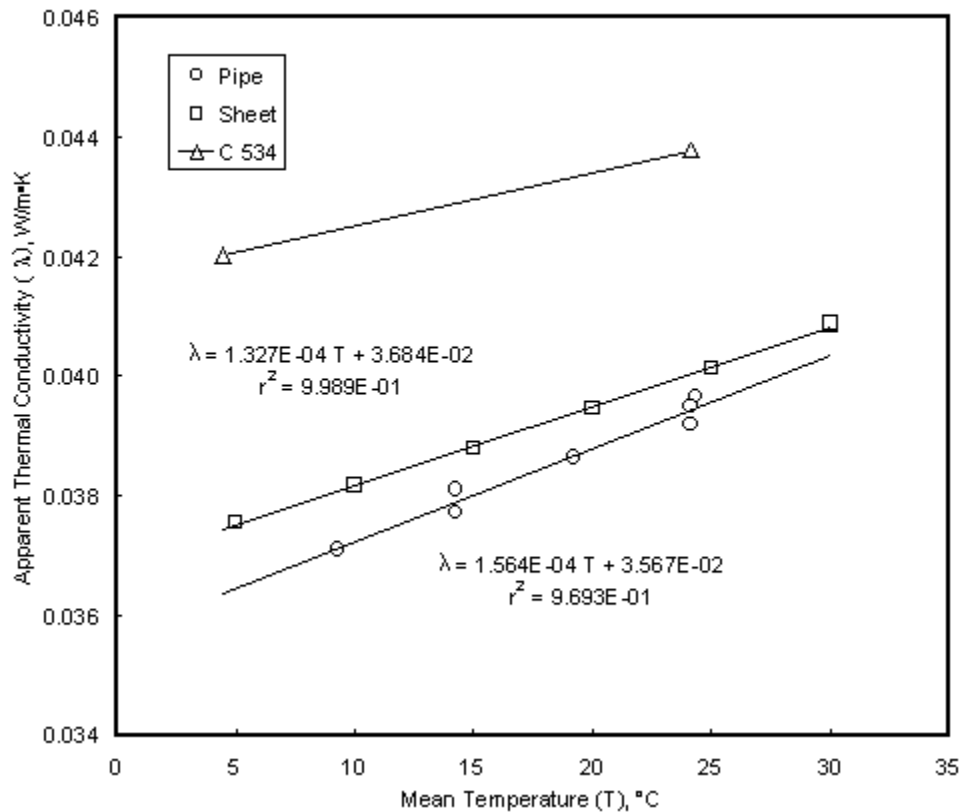


Figure 5 - Apparent Thermal Conductivity of Elastomeric Foam Insulation

Preformed Flexible Elastomeric Cellular Thermal Insulation in Sheet and Tubular Form (C 534). The regression curves for the two types of insulation agree within 1.5% and 2.5% at mean temperatures of 25 °C and 10 °C, respectively. This is considered good agreement, since the two materials are not identical. Also, the apparent thermal conductivities of both types of materials are well below the maxima allowed by C 534.

The test with the coldest pipe temperature, 0.6 °C, was performed on a day when our laboratory was especially dry, with the dew point temperature being about -1.6 °C. In our laboratory, achievement of this low a pipe temperature without condensation would usually require that the apparatus be placed within a dry enclosure. Our plan is to place the apparatus inside a commercially available glove box, where the dew point can be maintained as low as -76 °C by using molecular sieve desiccants. Specifications for such a glove box have been written and procurement is planned.

Design Modeling

The finite difference analysis of heat flow in the pipe insulation test apparatus has evolved during the course of this study. The initial efforts were focused on an investigation of the feasibility of the proof-of-concept hardware. Later analysis was used to further guide the design of the apparatus and related instrumentation.

Model Construction and Boundary Conditions

The first models were focused on the design parameters of the proof-of-concept equipment. Using this conceptual design, three series (designated Phase I, II, and III) of simple two-dimensional [radial (R) and axial (Z)], finite-difference models were created and run with the general-purpose heat conduction code HEATING.[3] The primary goal of this effort was to determine the level of accuracy that could be achieved within reasonable physical dimensions for the temperatures and materials of interest. Of particular concern was the influence of longitudinal heat transfer and the required thickness of the guard insulation.

Figure 6 shows the components included in the Phase I finite-difference models. The radial dimension is shown on the vertical axis and the axial dimension is shown on the horizontal axis. The cold pipe itself was not modeled, but was represented by a constant-temperature boundary condition. The boundary conditions on the ends and outer surfaces were those of natural convection to an environment at 23°C. The boundary condition on the centerline (left in Fig. 6) was one of symmetry. The guard insulation was assumed to have an apparent thermal conductivity of 0.06 W/m•K and a thickness of 25.4 mm (1.0 in.). The thin screen heater was taken to be 0.66 mm (0.026 in.) thick and to have an effective thermal conductivity of 2 W/m•K (1/7 that of solid nichrome). Nominal grid spacing in all of the models was 1 mm (0.04 in.) in the radial direction and 5 mm (0.20 in.) in the axial direction. The grid spacing was altered from the nominal values in order to accommodate the actual dimensions of components of the apparatus being modeled. The number of nodes in the models ranged from 3,978 to 27,233 in Phase I and from 10,890 to 58,743 in Phase II.

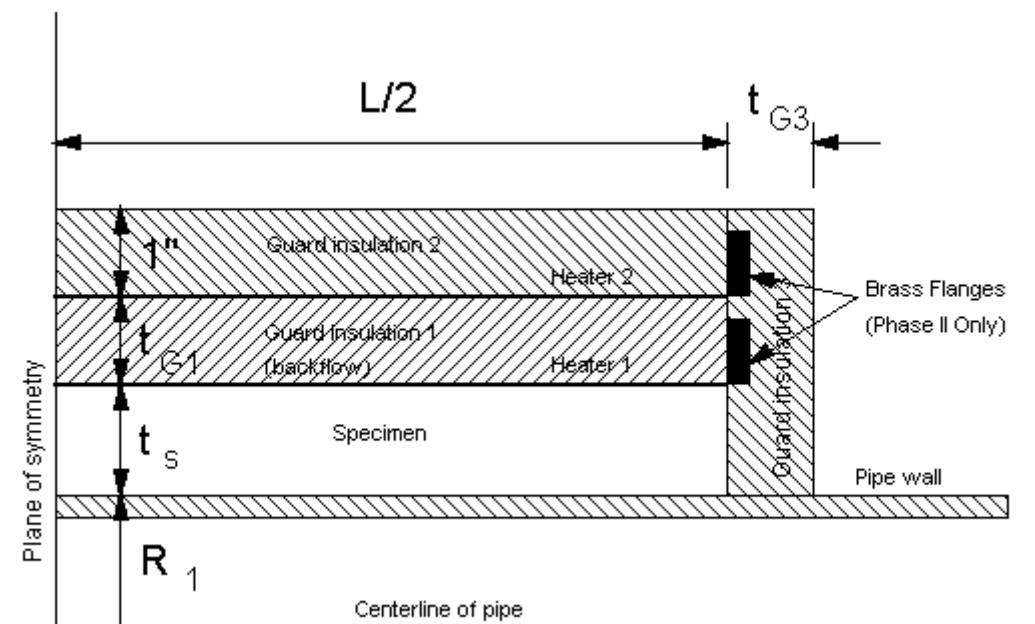


Figure 6 - Construction of Two-Dimensional (R-Z) Finite Difference Model

One important design consideration for the test apparatus is ensuring that all the heat produced by the thin screen heater flows through the test specimen. This is accomplished by placing a layer of guard insulation outside the screen heater and controlling the temperature on the other side of this guard to the same temperature as the screen heater. Then heat flow through this guard insulation is as close to zero as possible. In the Phase I and II models, it was assumed that this would be accomplished via the use of a second screen heater. In reality, the temperature will vary somewhat over the length of both heaters. In order to model the control scheme of the conceptual apparatus, the power level for the outer screen heater was selected by an iterative process in order to match the two heater temperatures at the center of the axial dimension (i.e., along the plane of symmetry) to within a very small tolerance (typically on the order of 0.01 °C or less). In the Phase III model, the second screen heater was replaced by a constant temperature boundary condition, representative of the heavy copper shell that had by then been constructed for the proof-of-concept test apparatus.

For each case, setting the first screen heater power level within the model was an iterative process. First the target temperature difference across the specimen was specified. In typical cryogenic applications the temperature difference will be large because the outside of the insulation will be at ambient conditions. In other situations, such as a pipe or tube carrying chilled brine, the temperature difference will be less. And in some of the initial proof-of-concept tests, the interior cold fluid temperature would be only slightly below room temperature. The cases modeled consider all these conditions. To ensure inward heat flow, even under near-room temperature conditions, a minimum temperature difference across the insulation specimen was set to 30 °C. Also, to ensure no inward heat flow from the environment across the heater, the heater temperature was set to no less than 2 °C above room temperature. In other words, the screen heater target temperature was set to equal the maximum of either: (1) the pipe temperature plus 30 °C, or (2) the room temperature plus 2 °C. Besides this target temperature, the pipe temperature, the specimen thickness, and the specified specimen apparent thermal conductivity were specified. One-dimensional radial heat flow across the insulation specimen was then calculated to determine the appropriate power level for the screen heater. This power level was then held fixed for the remainder of the calculations for that case.

Proof-of-Concept Calculations

Phase I of the finite difference analysis considered a broad range of possible insulation specimens and apparatus configurations. Table 2 shows the parameters that were varied during this and subsequent phases of the analysis effort. Most possible combinations of these variables were considered, resulting in about 500 cases. From each steady-state solution, the temperature of the thin-screen heater was used to represent the experimentally-measured temperature at the outer surface of the insulation specimen.

For all the cases shown in Table 2, the difference between the calculated and the input apparent thermal conductivities ranged from near-zero up to about 7% at these same thermocouple locations. The larger errors all occurred at the warmest interior fluid temperature of 20 °C and with the shortest pipe length of 0.5 m. The majority of the

results showed relatively flat temperature profiles on the screen heater to about midway between the midplane, or axis of symmetry, and the end of the apparatus. The deviation was larger for greater Guard 1 thicknesses. The effects of specimen conductivity lay within a relatively narrow band.

Table 2 - Finite difference model parameter values

Variable	Phase I		Phase II		Phase III
Radial Specimen dimensions (inner and outer diameters)	<i>(cm)</i>				
	ID	OD	ID	OD	
	1.9	8.9	same		same
	3.2	8.9	same		same
	7.6	12.7	same		same
			7.6	17.8	same
Specimen length	<i>(m)</i>				
	0.5				
	1.0		same		same
	1.5				
	2.0		same		same
			3.0		
Guard 1 thickness	<i>(cm)</i>				
	2.5		same		same
	5.1		same		same
Guard 3 thickness	0				
			5		
					10
	20				20
Specimen thermal conductivity	<i>(W/m•K)</i>				
	0.02		0.02		0.02
	0.04				
	0.06				
	0.08		0.08		0.08
Pipe temperature	<i>(°C)</i>				
	-200		same		same
	-30		same		same
	20		same		same

Apparatus Parametric Calculations

After considering these results, Phase II of the study was initiated. During this phase, several modifications were made to the model in order to more closely simulate the conceptual design and the hardware prototype that was under development. For example, the heavy brass flanges used to bring power in to the screen heaters were added, as was insulation covering these flanges. Also, larger pipe sizes and insulation thicknesses were added for this part of the analysis. These parameters are summarized in Table 2. The 3 m pipe length was examined only for the larger pipe diameters, since the first analysis had shown that shorter pipe lengths provided reasonable accuracy for the smaller pipe sizes.

Of major concern was the flatness of the temperature profile along the axis. As Figure 7 shows, this temperature varies along the axial dimension due to axial heat flow. Most cases were like those shown in Figure 7, with the temperature near the midplane relatively unaffected by the axial heat flow. The apparent thermal conductivity was calculated from Equation 1 using these temperatures, so that it also varies along the axial dimension. For the selected Phase II cases shown in Figure 7, and considering the thermocouple locations at 0.23 m from the midplane, the model predicts that the temperatures will be relatively unaffected by the axial heat flow and that the calculated apparent thermal conductivity will be within 0.2% of the 'true' value input to the model, even for insulation thicknesses up to 10 cm.

As described previously, thermocouples on the prototype apparatus were placed 0.23 m (9 in.) from the specimen center. To examine in more detail the effectiveness of the longitudinal passive guard arrangement protecting this metered section, calculated temperatures at locations at the center and 0.1, 0.2, and 0.3 m from the center were used for T_2 in Eqn. 1. The thermal conductivity calculated using temperatures at 0.2 and 0.3 m from the center were compared with the known thermal conductivity to derive estimates of the errors that will occur due to longitudinal conduction. The results from the Phase II analysis can be summarized in terms of the L/D parameter, that is, the length of the specimen divided by its outer diameter, as shown in Figure 8. Figure 8 shows:

- For $L/D < 5$, errors in thermal conductivity 0.3 m from the center cluster below 0.5% for cryogenic temperatures, rising to 3.5% for temperatures above room temperature. However, the errors 0.2 m from the center are smaller, with a maximum of 1% for temperatures above room temperature and smaller than 0.4% for temperatures less than $-30\text{ }^\circ\text{C}$. For a 1 m long specimen, these conditions would hold for outer diameters greater than 200 mm (7.9 in.).
- For $5 < L/D < 15$, errors in thermal conductivity 0.3 m from the center can be as high as 2.5% for room temperature tests, but are smaller than 0.4% for tests at $-30\text{ }^\circ\text{C}$ and $-200\text{ }^\circ\text{C}$. The errors 0.2 m from the center are again smaller, with a maximum of 0.45% at $20\text{ }^\circ\text{C}$ and smaller than 0.1% for $-30\text{ }^\circ\text{C}$ and colder. For a 1 m long specimen, these conditions would hold for outer diameters between 70 mm (2.6 in.) and 200 mm (7.9 in.).
- For $L \geq 2\text{ m}$, for the diameters and temperatures considered, no errors larger than 0.1% were noted.

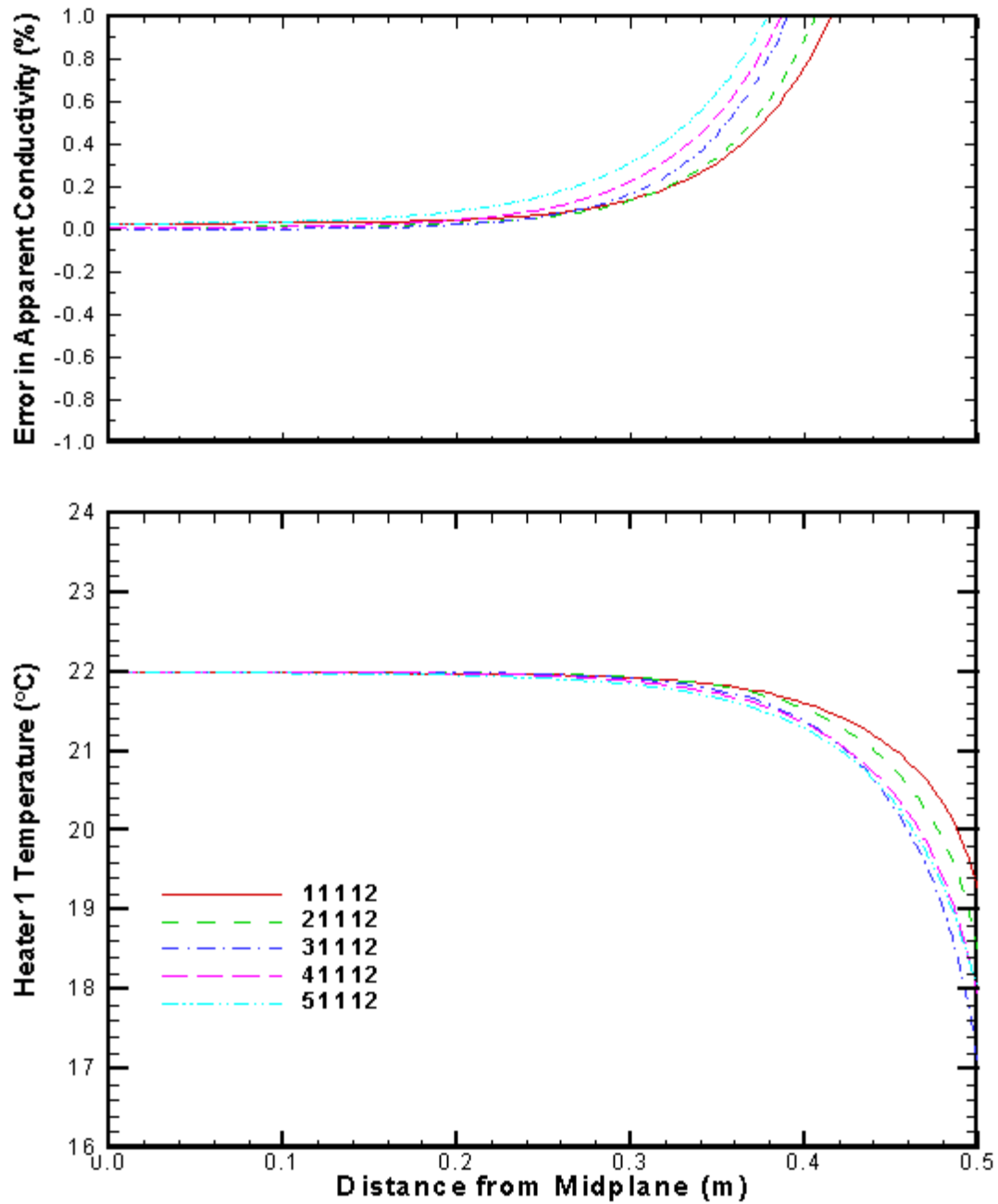


Figure 7 - Predicted heater temperatures and errors in apparent thermal conductivity along the test apparatus length, for a one meter long apparatus with 2.5 cm guard insulation thickness, 0.02 W/m•K specimen conductivity, -30 °C pipe temperature, and various specimen dimensions (ID/OD for curves 11112, 21112, 31112, 41112, and 51112, respectively): 1.9/8.9, 3.2/8.9, 7.6/12.7, 7.6/17.8, 15.2/35.6 cm.

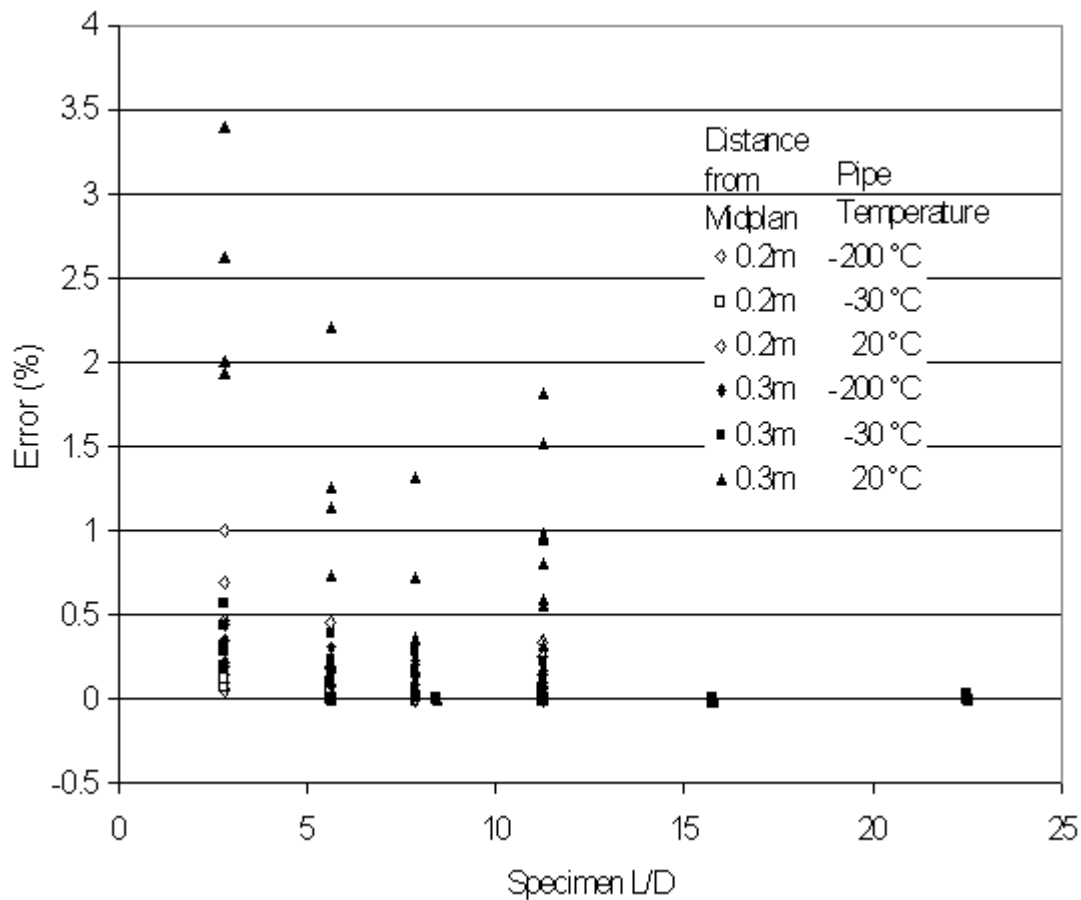


Figure 8 - Error in Thermal Conductivity Measurement due to Deviation from Pure Radial Heat Flow at Locations 0.2 and 0.3 m from the Midplane.

Based on an examination of the results, greater Guard 1 thicknesses reduce the accuracy of any measurements along the length of the pipe. Considering the results of these analyses, the prototype sub-ambient pipe insulation test apparatus should be equipped with a guard heater of no more than 25 mm (1-in.) thickness. Since the prototype will only examine specimens with a maximum outer diameter of 0.09 m (3.5 in.), giving a minimum L/D of 11, the accuracy associated with the apparatus geometry and material properties should be within $\pm 0.5\%$ (accuracy will be affected by other factors associated with instrumentation that are not considered here).

A Phase III analysis considered the improvements possible with thicker end guards and the replacement of the second screen heater and external guard with a constant temperature boundary condition. The results of these efforts were not significantly different from those presented for Phase II.

During initial trials with the proof-of-concept apparatus, several questions arose and were investigated using an expanded, three-dimensional version of the Phase II finite difference model previously created. These questions included possible geometric considerations associated with foam aging and the possible introduction of errors due to

the physical imperfections of any apparatus. A three-dimensional model was required for these studies because in each case the parameters varied in angular, radial, and axial directions.

One of the physical imperfections considered was the longitudinal seam in the screen heater. The use of a thin-screen heater wrapped around the test specimen allows accurate measurement of the heat input, but does require a seam where the two edges of the screen meet. The thermocouples are placed opposite this seam to minimize the effect of any imperfections, but there was a question about the possible magnitude of any errors the seam might cause in the test results. There are two possible seam defect configurations, first the screen edges could overlap slightly, causing an elevated heat production along the seam (and causing the average heat generation used in the calculations to overstate the heat production on the opposite side). Second, there could be a slight gap between the screen edges, causing a reduced heat production along the seam (and causing the average heat generation used in the calculations to understate the heat production on the opposite side).

Just as in the previous work, the physical parameters were varied in this study, as shown in Table 2 for Phase II. The seam imperfection was varied from a 7.5° gap to a 15° overlap, much larger than any expected defects. For a near-to-ambient cold-side temperature (shown previously to be one of the more challenging test conditions), with a 25 mm (1 in.) guard insulation thickness, the modeled temperature measurements opposite the seam were well within $\pm 1\%$ of those expected with a perfect seam, for all the seam descriptions considered.

Summary

A prototype apparatus for measurements of the apparent thermal conductivity of pipe insulation at temperatures below ambient has been constructed and demonstrated by measurements on specimens of three types of pipe insulation. Measurements on glass fiber insulation demonstrated the need to have a high emittance for the pipe. The measured conductivities were within 5% of the maxima allowed by C 547. Measurements on polyisocyanurate foam insulation were performed both on boards, using C 518, and on pipe-shaped insulation cut from the same material. The two types of measurements agreed within about 1% after aging of both materials had been nearly completed. Measurements on elastomeric foam insulation were also performed on sheet and tubular specimens, with agreement between the two methods being in the range of 1.5 to 2.5%. This level of agreement on these three types of insulation is considered to be a demonstration that the prototype apparatus is capable of accurate thermal conductivity measurements.

Measurements on the elastomeric foam insulation were extended down to a pipe temperature of 0.6 °C. This was accomplished without condensation because of the unusually low relative humidity in the laboratory during this test. Measurements with pipe temperatures this low or lower will generally require that the apparatus be placed within a low relative humidity enclosure to prevent condensation on the pipe or within the insulation. Plans are underway to acquire a glove box for this purpose. With the use of molecular sieve desiccants, dew point temperatures as low as -76 °C (-105 °F) can be maintained.

A finite-difference model of the prototype apparatus was used to explore the effect of longitudinal heat transfer on the measured temperature. This model predicts that the specimen's apparent thermal conductivity calculated using measured temperatures should be within $\pm 0.5\%$ of the true value.

It is suggested that this type of apparatus be included in C 335, and that manufacturers produce this type of equipment.

References

- [1] Nextel is a high emittance paint manufactured by the 3M Company.
- [2] McElroy, D. L., Graves, R. S., Yarbrough, D. W., and Moore, J. P., "A Flat Insulation Tester That Uses an Unguarded Nichrome Screen Wire Heater," *Guarded Hot Plate and Heat Flow Meter Methodology, ASTM STP 879*, C. J. Shirliffe and R. P. Tye, Eds., American Society for Testing and Materials, Philadelphia, 1985, pp. 121-139.
- [3] Childs, K. W., Heating 7.2 User's Manual, ORNL/TM-12262, Oak Ridge National Laboratory, Oak Ridge, Tennessee, February 1993.

Acknowledgement

Funding for this project was provided by the U.S. Department of Energy, Office of Building Technology, State, and Community Programs under contract number DE-AC05-00OR22725 with the Oak Ridge National Laboratory, managed by UT-Battelle, LLC.